Nuclear Spin and Magnetic Hyperfine Interaction of 12-Day Ge^{71}†

W. J. CHILDS AND L. S. GOODMAN
Argonne National Laboratory, Argonne, Illinois
(Received 7 March 1963)

The hyperfine structure of the ^3P atomic ground state of radioactive Ge^{71} has been examined by means of the atomic-beam magnetic-resonance technique. The nuclear spin and magnetic dipole moment are measured to be $\frac{1}{2}$ and $+0.65\pm0.20$ nm, respectively. The magnetic hyperfine interaction constants $a(^3P_1)$ and $a(^3P_2)$ are found to be $\pm(87.005\pm0.003)$ and $\pm(357\pm6)$ Mc/sec, respectively. The electronic g factor g_J is determined to be 1.50093 ± 0.00008 for the $^3P_1$ state and 1.4948 ± 0.0007 for the $^3P_2$ state.

INTRODUCTION

SINCE all but one of the stable isotopes of germanium ($Z=32$) are even-even, the radioactive odd-A nuclei must be studied in order to investigate the filling of the neutron shells in this region.

When germanium is irradiated in a flux of thermal neutrons, three odd-neutron germanium isotopes of convenient lifetimes can be produced: Ge^{71}(12 day), Ge^{75}(82 min), and Ge^{77}(12 h). No nuclear spins or moments have previously been determined for these isotopes. The use of such a source in an atomic-beam magnetic-resonance machine should permit a complete investigation of these properties. The present research was undertaken to obtain these measurements. This report is concerned with results on the 12-day isotope, Ge^{71}.

PRINCIPLE OF THE METHOD

The basic principle of the atomic-beam magnetic-resonance technique of Rabi[1] and Zacharias[2] is now classic, and accordingly only a very brief account will be given here. Neutral atoms of the beam, after emerging from a well-defined source (Fig. 1), pass in turn through three magnetic fields (conventionally designated, in order of passage, by the letters A, C, B) and, after passing through a thin slit, strike a detector. The A and B fields are strong and inhomogeneous, and (in the scheme of Zacharias) have their gradients in the same direction. Each atom of the beam is normally deflected in the same sense in the two inhomogeneous fields and can reach the detector only if its effective magnetic moment is reversed in sign in the C region. This can be accomplished in the homogeneous C field by permitting the atom to interact with a radio-frequency field whose frequency corresponds (by the Planck condition) to the transition energy required for the reversal of the high-field effective moment. The energy levels are sharply defined and a measure of the resonant frequencies for known values of the homogeneous field can give information on a number of parameters. A more complete discussion will be found in the section labeled Theory.

PREPARATION OF THE RADIOACTIVE SOURCE

The Ge^{71} sources were prepared by irradiating 1-g chunks of germanium metal in the Argonne research reactor CP-5 for 1–2 weeks at a flux of 2×10^{13} neutrons-cm^{-2}-sec^{-1}. The germanium chunks were irradiated in the graphite oven subsequently used in the atomic-beam machine in order to reduce the exposure of personnel. Since there are no gamma rays associated with Ge^{71}, a thin shield offered effective protection once the 12-h Ge^{77} had decayed.

EXPERIMENTAL DETAILS

Oven and Alignment of the Beam

Graphite was found to be a satisfactory oven material for production of the germanium atomic beam. At a temperature of about 1500°C, produced by electron bombardment of the oven mount, an adequate beam of radioactive Ge^{71} could be detected.

Since accurate alignment of the oven was essential, it was necessary to have some method of detecting atoms coming from the oven slit. Unfortunately, no such detector for stable germanium atoms was available. Although radioactive Ge^{71} atoms could be detected by means of their radioactivity, this procedure was not suitable for critical alignment of the beam. Stable gallium metal was accordingly added to the oven load

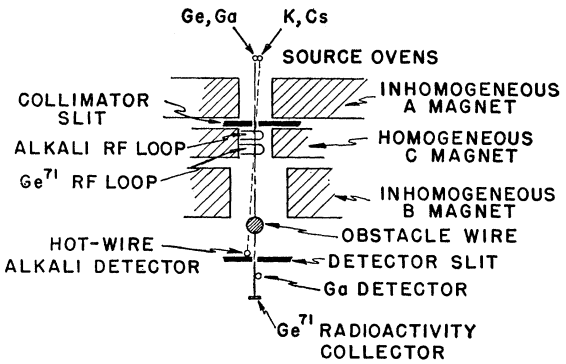

FIG. 1. Schematic diagram of the atomic-beam magnetic-resonance apparatus. The auxiliary equipment used in connection with the alkali calibration beam is indicated. The slits, Ge-Ga oven, obstacle wire, and both surface ionization detectors are adjustable for both lateral and tilt motion.

† Work performed under the auspices of the U. S. Atomic Energy Commission.

[1] I. I. Rabi, J. R. Zacharias, S. Millman, and P. Kusch, Phys. Rev. **53**, 318 (1938).

[2] J. R. Zacharias, Phys. Rev. **61**, 270 (1942).

after irradiation since it can be readily detected with an oxidized hot tungsten wire. The gallium beam could thus be used for alignment of the oven, calibration of the homogeneous magnetic field, and for positioning of the obstacle wire. It was normally necessary to add gallium to the oven load prior to each run.

Since germanium has integral electronic angular momentum in its atomic ground state ($J=0$, 1, and 2), many atoms will pass through the inhomogeneous magnetic fields with m_J, the z component of the total electronic angular momentum, equal to zero. Since the effective magnetic moment of such atoms is zero, they will suffer no magnetic deflections and some will pass along the machine axis and strike the detector. The obstacle wire is positioned so as to limit the background of such atoms reaching the detector. It also reduces the number of very fast atoms (with small deflections) which can reach the detector. It is, thus, very effective in reducing the nonresonant signal strength.

Calibration of the Homogeneous Magnetic Field

A second oven, placed a little above and to one side of the germanium-gallium oven, was used to produce a beam of potassium and cesium atoms. The alkali beam, detected by an off-center surface-ionization detector, was then used for calibration of the homogeneous field. Since the C field contained two rf loops, suitable resonance transitions could be induced simultaneously in both the Ge^{71} and the alkali (but at different frequencies). To measure any possible field difference between the two loop positions, the alkali resonance used for calibration was observed by use of both loops in turn, and any frequency difference was noted. The difference never amounted to more than 14 kc/sec, and in any case could be quantitatively corrected for.

Toward the end of the experimental work, the alkali oven load was depleted so that it was no longer usable. Reloading the oven would have necessitated a time-consuming reclamation operation because of the high radiation level in the vacuum system of the oven. (The most troublesome activity was from 49-day In^{114m} used in a previous experiment.) Consequently, a different method of field calibration was used. The gallium beam from the germanium oven was detected by the on-center oxidized hot tungsten wire detector and used for calibration. To permit Ge^{71} atoms to continue past the gallium detector and strike the radioactivity collector, however, it was necessary to move the wire out of the beam until some of the beam still hit the wire but most passed by to the Ge^{71} detector. The detector wire was not moved aside until all alignment procedures had been completed.

Detection of the Radioactive Ge^{71}

As noted above, the Ge^{71} beam was detected by means of its radioactivity. The beam was allowed to fall on small copper-coated steel collectors which could subsequently be removed from the vacuum system and counted. A normal "run" consisted in collecting for ten 4-min periods, each on a different collector and at a slightly different rf frequency. The rf spectrum of Ge^{71} was then shown by the activity of the collectors as a function of frequency for the particular intensity of the homogeneous field used. Further details of the collection system have been published.[3]

THEORY

Transition Frequencies and the Nuclear Spin

The electronic configuration of nonexcited germanium is $4p^2$. The atomic ground state is, thus, $^3P_{0,1,2}$ with the $^3P_0$ lying lowest. The separations of these states are sufficiently small that atoms in all three states may be expected at the temperature of the atomic beam. The relative populations of these states in a beam have been measured,[4] and the electronic g factors for the $^3P_1$ and $^3P_2$ states have been precisely obtained.[4] The Hamiltonian describing the nuclear and electronic interactions is given[5] by

$$\mathcal{H}=ha\mathbf{I}\cdot\mathbf{J}+hbQ_{\text{op}}+g_J\mu_0H(J_z+\gamma I_z), \qquad (1)$$

where terms through the quadrupole interaction have been retained. The nuclear spin I and the total electronic angular momentum J are related to their respective dipole moments by the relations $\mu_J=-g_J\mu_0J$ and $\mu_I=-g_I\mu_0I$. The moments are, thus, defined in terms of the angular momenta, the g factors, and the Bohr magneton μ_0. The ratio of the nuclear g factor g_I to the electronic g factor g_J is γ. The external field (along the z axis) is denoted by H, and h is Planck's constant. The parameters a and b are to be determined experimentally, and the electric-quadrupole-interaction operator Q_{op} is defined in reference 5.

At a sufficiently small value of the external magnetic field, the eigenvalues may be evaluated by first-order perturbation theory. The energy differences between pairs of states that have equal but opposite effective magnetic moments at strong field (the refocusing condition) may then be expressed as functions of the unknown parameters I, a, and b to a very good approximation. Of these transitions, only those that satisfy the selection rules $\Delta F=0$, ±1 and $\Delta m_F=0$, ±1 are normally of interest. Because of the fact that J for germanium is integral rather than half-integral, however, it is seen that the only transitions satisfying the conditions above are characterized by $\Delta F=\pm1$. Such transitions have resonance frequencies which depend, even at zero field, directly on the unknown parameters

[3] W. J. Childs, L. S. Goodman, and L. J. Kieffer, Phys. Rev. **120**, 2138 (1960).
[4] I. Bender, thesis, Erstes Physikalischen Institut, University of Heidelberg (unpublished).
[5] N. F. Ramsey, *Molecular Beams* (Oxford University Press, New York, 1956), p. 272.

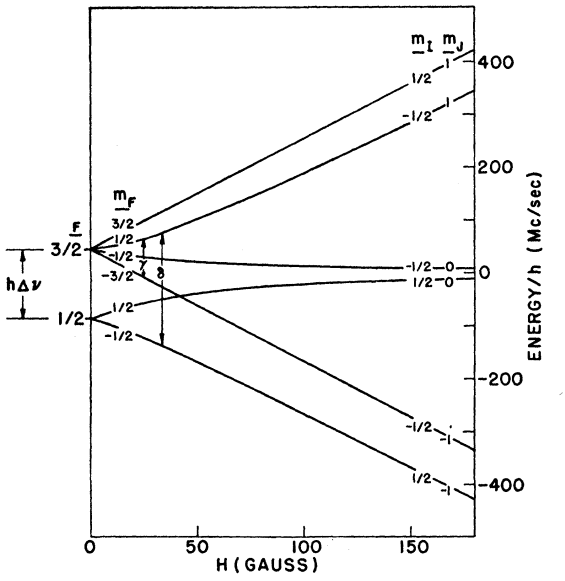

FIG. 2. Hfs diagram for the lowest $^3P_1$ atomic state of Ge^{71}. The transitions observed (γ and δ) are shown. The magnetic hyperfine interaction constant a has been assumed positive.

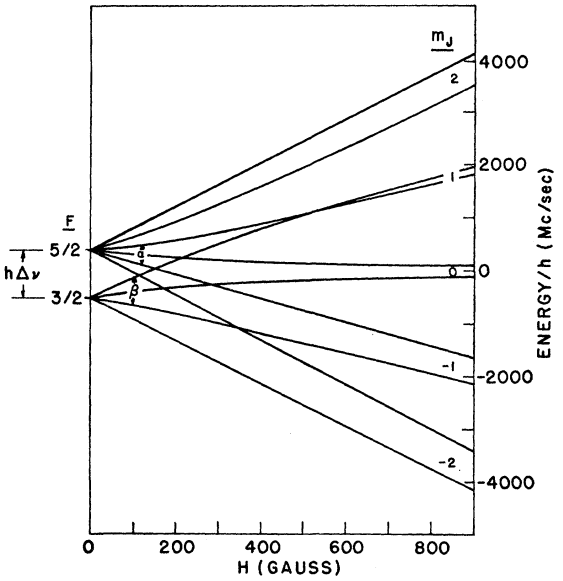

FIG. 3. Hfs diagram for the lowest $^3P_2$ atomic state of Ge^{71}. The transitions observed (α and β) are indicated. The magnetic hyperfine interaction constant a has been assumed positive.

a and b, however; and it was, therefore, impractical to search for them with the radioactivity collector.

Figure 2 shows the hfs diagram for the $^3P_1$ state with, for example, a nuclear spin $I=\frac{1}{2}$. Transition δ is of the type discussed and would be difficult to observe without accurate knowledge of a. Transition γ satisfies the refocusing condition, has a transition frequency that is independent of a at low field, but does not obey the selection rules. Atoms can, however, be made to undergo transitions of this type in a two-quantum process with a resonance frequency given by

$$\nu=\frac{E\text{ (upper level)}-E\text{(lower level)}}{2h}.$$

If the interaction of the external field with the nuclear dipole moment is ignored in comparison with the interaction with the electronic moment, the double-quantum transition frequency at low field may be expressed (by first-order perturbation theory) as a function of the nuclear spin I. Thus, for $^3P_1$ atoms, the relation is

$$\nu_\gamma\approx\frac{g_J\mu_0 H}{(I+1)h}. \tag{2}$$

Similarly, for $^3P_2$ atom , transitions α and β (shown in Fig. 3) have the frequencies

$$\nu_\alpha\approx\frac{2g_J\mu_0 H}{(I+2)h}, \tag{3}$$

and

$$\nu_\beta\approx\frac{g_J\mu_0 H(I+4)}{(I+1)(I+2)h}. \tag{4}$$

A systematic search at low fields quickly revealed resonances in both the $^3P_1$ and $^3P_2$ states, but only at those frequencies consistent with a nuclear spin $I=\frac{1}{2}$.[6]

The Nuclear Magnetic Dipole Moment

The problem is greatly simplified once the nuclear spin is shown to be $\frac{1}{2}$. In the first place, the second term in the Hamiltonian vanishes because the quadrupole interaction is not observable for $I<1$. In addition, the largest matrix occurring in the secular determinant is only 2×2, so that an explicit solution for all eigenvalues may readily be found. Thus, the general expression for all eigenvalues is

$$E(J\pm\tfrac{1}{2},\,m_F)=\frac{ah}{2}\left\{-\tfrac{1}{2}+2m_F x\pm\left[\left(\frac{2J+1}{2}\right)^2-2m_F(1-\gamma)x+(1-\gamma)^2x^2\right]^{1/2}\right\}, \tag{5}$$

where the dimensionless parameter x signifies[7]

$$x=\frac{g_J\mu_0 H}{|a|h}.$$

Figure 3 shows the hfs diagram for the $^3P_2$ atomic state. (The justification for the assumption of a positive

[6] W. J. Childs and L. S. Goodman, Bull. Am. Phys. Soc. **5**, 411 (1960).

[7] Equation (5) gives the eigenvalues of the Hamiltonian of Eq. (1) exactly, and the measurement of μ_I depends on this exactness. It should be noted that our definition of x, though slightly unconventional, is the one required in Eq. (5).

nuclear magnetic dipole moment will be discussed below.) From Eq. (5), the double-quantum transitions labeled α and β have resonance frequencies of

$$\nu_\alpha \equiv \frac{E(\tfrac{5}{2},\tfrac{1}{2})-E(\tfrac{5}{2},-\tfrac{3}{2})}{2h}$$
$$= ax+\tfrac{5}{8}a\left\{\left[1-\frac{4}{25}(1-\gamma)x+\frac{4}{25}(1-\gamma)^2x^2\right]^{1/2} -\left[1+\frac{12}{25}(1-\gamma)x+\frac{4}{25}(1-\gamma)^2x^2\right]^{1/2}\right\}, \quad (6)$$

and

$$\nu_\beta \equiv \frac{E(\tfrac{3}{2},\tfrac{3}{2})-E(\tfrac{3}{2},-\tfrac{1}{2})}{2h}$$
$$= ax-\tfrac{5}{8}a\left\{\left[1-\frac{12}{25}(1-\gamma)x+\frac{4}{25}(1-\gamma)^2x^2\right]^{1/2} -\left[1+\frac{4}{25}(1-\gamma)x+\frac{4}{25}(1-\gamma)^2x\right]^{1/2}\right\}, \quad (7)$$

respectively. The double-quantum transition γ, shown in the hfs diagram for the $^3P_1$ atomic state (Fig. 2), has the frequency

$$\nu_\gamma \equiv \frac{E(\tfrac{3}{2},\tfrac{1}{2})-E(\tfrac{3}{2},-\tfrac{3}{2})}{2h}$$
$$= \frac{ax}{4}(3+\gamma)+\tfrac{3}{8}a\left\{\left[1-\frac{4}{9}(1-\gamma)x+\frac{4}{9}(1-\gamma)^2x^2\right]^{1/2}-1\right\}, \quad (8)$$

where the quantum numbers in parentheses refer to the appropriate values of F and m_F for the zero-field state from which the state in question is adiabatically derived. While F is a good quantum number only at zero field, the expressions given above are valid at any field.

In a later phase of the work, transition δ in Fig. 2 was observed. Its resonance frequency, again from Eq. (5), is

$$\nu_\delta \equiv \frac{E(\tfrac{3}{2},\tfrac{1}{2})-E(\tfrac{1}{2},-\tfrac{1}{2})}{h}$$
$$= ax+\tfrac{3}{4}a\left\{\left[1-\frac{4}{9}(1-\gamma)x+\frac{4}{9}(1-\gamma)^2x^2\right]^{1/2} +\left[1+\frac{4}{9}(1-\gamma)x+\frac{4}{9}(1-\gamma)^2x^2\right]^{1/2}\right\}. \quad (9)$$

Once the nuclear spin has been determined, the only unknown parameters on which these transition frequencies depend are the magnetic dipole moment (through γ) and the magnetic hyperfine-interaction constant a. All four transition frequencies depend much more strongly on a than on γ. For this reason, good values for the interaction constants $a(^3P_1)$ and $a(^3P_2)$ were obtained first. Observations at strong fields were required to give even a crude result for the nuclear dipole moment μ_I.

Additional Comments on the Multiple-Quantum Transitions

Multiple-quantum transitions possess a number of characteristics that can cause the experimentalist some difficulty. The rf power required to induce such transitions generally increases rapidly as increasing field strength causes the resonance frequency to deviate from the Zeeman spacings. This is not too troublesome if rf signals of adequate strength are available. Applying too much power to the transition may introduce error, however, by shifting the observed frequency for optimum resonance signal somewhat off the true resonant frequency. In the present experiment, such shifts were apparent on several occasions and were eliminated by subsequent runs at reduced rf power levels. The best evidence that the present figures do not contain appreciable systematic errors of this sort is their internal consistency.

OBSERVATIONS AND RESULTS

The details of all the observations are listed in Table I. The transitions observed ($\alpha,\beta,\gamma,\delta$) are indicated in Figs. 2 and 3. Transition γ has a small dependence on μ_I at all fields, but depends strongly on g_J and $|a|$. Since a good value for g_J was available,[4] this transition was used to provide a close estimate of the zero-field hyperfine interval $\Delta\nu(^3P_1)$. After transition γ was observed at 30 G, it was possible to estimate $\Delta\nu(^3P_1)$ to be 130.3±0.3 Mc/sec. A search in this region, at 0.15 G, revealed the single-quantum $\Delta F=\pm1$ transition δ (Fig. 4), which at this field has only a very weak dependence on μ_I and g_J. Several runs under these conditions gave an accurate determination of $|a|$, namely,

$$|a(^3P_1)| \equiv \tfrac{2}{3}\Delta\nu(^3P_1)=87.005\pm0.003 \text{ Mc/sec}.$$

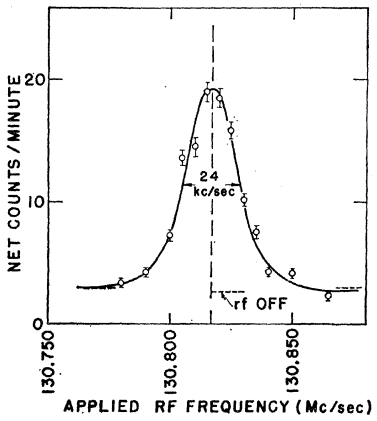

FIG. 4. Transition δ (in the $^3P_1$ atomic state) as observed at a field of 0.146 G. The calculated displacement of the resonance from its zero-field position is +309 kc/sec. The three dashed lines show three measurements of the relative intensity with the rf off.

TABLE I. Summary of observations on Ge^{71}. All frequencies are in Mc/sec except in the last column, where the frequency differences are given in kc/sec. The transitions used for field calibration were $Cs^{133}(4, -3 \leftrightarrow 4, -4)$; $K^{39}(2, -1 \leftrightarrow 2, -2)$; and the $(2, 0 \leftrightarrow 2, -1)$ transition in the metastable $P_{3/2}$ state of Ga^{69}. The electronic g factors used in calculating the calibration frequencies are those compiled by Hughes.[a] The value given in the first column for the magnetic field is that at the position of the loop used for the Ge^{71} transitions. The field at the calibration loop was, in some cases, different by as much as 10 mG. The calibration frequency in column 3 gives the frequency required at the calibration loop in order to assure the stated field at the Ge^{71} loop. The number N gives the number of quanta involved in the Ge^{71} transition. The values of g_J, a, and μ_I used to calculate the theoretical Ge^{71} transition frequencies are those listed in Table II.

H (G)	Calibration isotope	Calibration frequency	Ge^{71} transition	J	N	F	Observed Ge^{71} frequency	$\nu_{calc}-\nu_{obs}$
1	Cs^{133}	0.350	β	2	2	3/2	2.499±0.010	11
20	Cs^{133}	7.035	α	2	2	5/2	33.550±0.015	−3
39	Cs^{133}	13.789	α	2	2	5/2	65.598±0.015	−5
52	Cs^{133}	18.450	α	2	2	5/2	87.649±0.006	−13
70	Cs^{133}	24.958	α	2	2	5/2	118.333±0.005	−3
3	K^{39}	2.130	γ	1	2	3/2	4.223±0.015	12
5.989	K^{39}	4.320	γ	1	2	3/2	8.522±0.005	3
10	K^{39}	7.334	γ	1	2	3/2	14.392±0.004	5
15	K^{39}	11.258	γ	1	2	3/2	21.906±0.005	3
21	K^{39}	16.208	γ	1	2	3/3	31.215±0.010	2
30	K^{39}	24.149	γ	1	2	3/2	45.777±0.005	4
130	Ga^{69}	176.220	γ	1	2	3/2	237.333±0.015	−10
0.146	$Ga^{69,71}$	0.140	δ	1	1	3/2 ↔ 1/2	130.817±0.005	−2
0.15	K^{39}	0.105	δ	1	1	3/2 ↔ 1/2	130.820±0.006	3
0.15	K^{39}	0.105	δ	1	1	3/2 ↔ 1/2	130.820±0.009	3
80	Ga^{69}	92.129	δ	1	1	3/2 ↔ 1/2	378.053±0.020	−9
130	Ga^{69}	176.205	δ	1	1	3/2 ↔ 1/2	573.305±0.020	4

[a] V. W. Hughes, in *Recent Research in Molecular Beams*, edited by I. Estermann (Academic Press Inc., New York, 1959), pp. 87–90.

With this accurate value of $|a|$, further observations of transitions γ and δ at stronger fields were analyzed to give information on μ_I and g_J. The final results are

$$\mu_I = +0.65 \pm 0.20 \text{ nm},$$
$$g_J(^3P_1) = 1.50093 \pm 0.00008.$$

Transition α, in the $^3P_2$ state, was observed at fields up to 70 G. At these fields, the transition frequency depends strongly on $|a(^3P_2)|$ and $g_J(^3P_2)$, and less strongly on μ_I. From the value obtained for μ_I from the $^3P_1$ data, a simultaneous fit of the $^3P_2$ data for $|a|$ and g_J gave the results

$$|a(^3P_2)| = 367 \pm 15 \text{ Mc/sec},$$
$$g_J(^3P_2) = 1.4948 \pm 0.0007.$$

Since this value for g_J is less precise than that of reference 4, the latter value (1.4943 ± 0.0002) was used to refine the value given for $|a|$. The result is

$$|a(^3P_2)| = 357 \pm 6 \text{ Mc/sec}.$$

All of the results are given in Table II.

Calculation of $|\mu_I|$ from Measured Value of $|a(^3P_2)|$

The magnitude of the nuclear magnetic moment has been calculated from the measured $^3P_2$ hfs value by use of the method of Trees.[8] The value of ζ was taken[9] to be 880 cm^{-1}. The value thus obtained is

$$|\mu_I| = 0.60 \text{ nm}.$$

It was also calculated relativistically by the method of Schwartz.[10] The value obtained in this way is

$$|\mu_I| = 0.62 \text{ nm}.$$

These calculations are somewhat sensitive (3%) to the effective nuclear charge assumed. The value calculated may also be in error by some small amount because of configuration interaction which has not been taken into account. A fairly generous estimate of these uncertainties leads to the result

$$|\mu_I| = 0.62 \pm 0.06 \text{ nm}.$$

The calculation shows that the ratio $a(^3P_2)/\mu_I$ is positive, and since μ_I is measured to be positive it may be concluded that $a(^3P_2)$ is positive. It should be em-

TABLE II. Results for the atomic and nuclear properties of Ge^{71}.

Atomic state	$^3P_1$	$^3P_2$
J	1	2
g_J (Present results)	1.50093±0.00008	1.4948± 0.0007
g_J (From reference 4)	1.5009 ±0.0002	1.4943± 0.0002
$\|a\|$ (Mc/sec)	87.005 ±0.003	357 ± 6
$\Delta\nu$ (Mc/sec)	130.508 ±0.005	893 ±15

Nuclear Properties $I = \frac{1}{2}$

Nuclear magnetic dipole moment, μ_I	Method used
+0.65±0.20 nm	Direct measurement
±(0.62±0.06) nm	Theoretical deduction from measured value for $\|a(^3P_2)\|$.

[8] R. Trees, Phys. Rev. **92**, 308 (1953).
[9] E. U. Condon and G. H. Shortley, *Theory of Atomic Spectra* (Cambridge University Press, New York, 1951).
[10] C. Schwartz, Phys. Rev. **97**, 380 (1954).

phasized, however, that the absolute sign of the hyperfine interaction was not measured for either atomic state in the present experiment.

DISCUSSION

The measured nuclear spin $I=\frac{1}{2}$ for Ge^{71}, while entirely consistent with the nuclear shell model, could not be theoretically predicted with confidence because of closely competing orbits. The simplest interpretation is that the angular momentum is due entirely to the odd neutron in the $^3p_{1/2}$ orbit. The shell-model magnetic dipole moment expected from this configuration is $+0.64$ nm, in close agreement with both the measured value of $+0.65\pm0.20$ nm and the value $\pm(0.62\pm0.06)$ nm deduced theoretically from the measured value of $a(^3P_2)$.

ACKNOWLEDGMENT

One of the authors (L.S.G.) would like to thank G. Nöldeke, now at the Institut für Kernphysik der Universität Mainz, for his help and advice with the moment calculation during the former's stay as a Guggenheim Fellow at the University of Heidelberg (1960–1961).

PHYSICAL REVIEW VOLUME 131, NUMBER 1 1 JULY 1963

Electronic Polarizabilities and Sternheimer Shielding Factors

R. E. WATSON*
Atomic Energy Research Establishment, Harwell, England and Bell Telephone Laboratories, Murray Hill, New Jersey

AND

A. J. FREEMAN†
U. S. Army Materials Research Agency, Watertown Massachusetts and National Magnet Laboratory,‡ Massachusetts Institute of Technology, Cambridge, Massachusetts

(Received 4 March 1963)

A new method is developed for determining the distortions (polarizabilities) induced in electronic distributions by valence electrons and/or crystalline fields and their effect (expressed as Sternheimer shielding factors) on magnetic and electric hyperfine interactions. For illustrative purposes emphasis is placed in this paper on the calculation of Sternheimer antishielding factors (γ_∞). Working within the framework of the Hartree-Fock self-consistent field formalism, it is shown that the 'angular' excitations are gotten by relaxing the usual restriction that the spatial part of the one-electron functions be separable into a radial function times an angular function; relaxing the restriction that electrons of the same shell but differing in magnetic quantum number (m_l) have the same radial function yields the 'radial' excitations. To illustrate the method, calculations are reported for several spherical ions (Cl^- and Cu^+) in an external field, but the scheme is also applicable to the problem of induced electric quadrupole (and magnetic dipole and higher multipole) distortions of an ion by its own aspherical charge distribution. The problems of orthogonality, exchange, and self-consistency, which have complicated applications of the perturbation method are easily resolved by this approach. Further, since a self-consistent field procedure is followed, the distortions induced in the inner closed shells by the distorted outer shells are included in a natural way and by comparison with the results of the perturbation-variation method (which does not take these into consideration) these additional effects are shown to be significant.

I. INTRODUCTION

ELECTRIC quadrupole and magnetic dipole interactions between atomic nuclei and outer electron distributions have been measured in atoms and molecules, and in metals and salts by a variety of methods and most recently by recoilless emission and absorption of γ rays (the Mössbauer effect). As emphasized by Sternheimer,[1] the interpretation of these experiments (such as the measurement of the nuclear quadrupole moment Q) is complicated by the contributions to the hyperfine interactions arising from the distortion of the otherwise spherical closed electronic shells of the system. One of Sternheimer's important contributions was the striking demonstration that, for an ion having a nuclear quadrupole moment, the quadrupole interaction arising from the field induced (1) by external charges (as in a salt) or (2) from the ion's own aspherical charge distribution (if the ion is not spherically symmetrical) was changed appreciably by the distortion

* Present address: Bell Telephone Laboratories, Murray Hill, New Jersey; part of the work of this author was done while on a National Science Foundation postdoctoral fellowship.
† Present address: National Magnet Laboratory, Massachusetts Institute of Technology, Cambridge, Massachusetts.
‡ Supported by the Air Force Office of Scientific Research.
[1] R. M. Sternheimer, Phys. Rev. **80**, 102 (1950); **84**, 244 (1951); **96**, 951 (1954); **107**, 1565 (1957); **115**, 1198 (1959); **123**, 870 (1961); **127**, 812 (1962); R. M. Sternheimer and H. M. Foley, *ibid.* **92**, 1460 (1953). H. M. Foley, R. M. Sternheimer, and D. Tycko, *ibid.* **93**, 734 (1954).